Analytical Methods

PAPER

View Article Online
View Journal | View Issue

Published on 04 January 2016. Downloaded by Universita Studi di Milano on 28/01/2016 14:32:42.

Cite this: *Anal. Methods*, 2016, **8**, 1103

Development of an electrochemical nanosensor for the determination of gallic acid in food

Masoud Ghaani,[ab] Navid Nasirizadeh,*[ac] Seyed Ali Yasini Ardakani,[a] Farzaneh Zare Mehrjardi,[a] Matteo Scampicchio[d] and Stefano Farris[b]

Received 16th October 2015
Accepted 23rd December 2015

DOI: 10.1039/c5ay02747k

www.rsc.org/methods

In the present work, a silver nanoparticle/delphinidin modified glassy carbon electrode (AgNP/Delph/GCE) was fabricated as a highly sensitive electrochemical sensor for gallic acid (GA) determination. Cyclic voltammetry experiments indicated a higher sensitivity and better selectivity for gallic acid when using the AgNP/Delph/GCE as compared with the bare GCE surface, which were attributed to AgNPs and delphinidin, respectively. Moreover, the calculated surface electron transfer rate constant (k_s), and the electron transfer coefficient (α) between the GCE and the electrodeposited delphinidin demonstrated that delphinidin is an excellent electron transfer mediator for the electrocatalytic process. The average catalytic rate constant (k') of the overall process was also estimated to be 7.40×10^{-4} cm s^{-1} for the AgNP/Delph/GCE in the presence of 1.50 mmol L^{-1} of GA. Amperometry experiments were used to determine the limit of detection of the AgNP/Delph/GCE electrochemical sensor, which was 0.28 μmol L^{-1} of GA. Finally, two linear ranges were found, *i.e.* 0.60–8.68 μmol L^{-1} and 8.68–625.80 μmol L^{-1} for GA. The activity of the modified electrode was eventually investigated to assess the potential quantification of GA in real foods.

1. Introduction

Phenolic compounds are strong antioxidants present in different kinds of plants and fruits such as bananas, citrus fruits, and tea. These compounds have captured great attention in recent years due to both scavenging ability against free radicals and ready availability.[1–3] Phenolic acids represent one of the main subsets of phenolic compounds.[4] The main types of phenolic acids in plants include hydroxycinnamic acid derivatives, such as caffeic acid, ferulic acid, and hydroxybenzoic acid derivatives, *e.g.* vanillic acid and gallic acid.[5]

Gallic acid (GA), in particular, is one of the most important phenolic components found in bananas, blueberries, cantaloupes, grapes, and several other fruits. Previous studies have shown different properties belonging to GA, namely anti-carcinogenic, anti-mutagenic, and antioxidant properties.[6] For these reasons, GA and its esters have found an extensive use as additives in several sectors, especially cosmetics and food industry.[7,8] Over the last decade, fine quantification of GA in different systems has become one of the main research topics in analytical chemistry, whereby new detection techniques are sought-after.[9] The most established methods to quantify GA and other phenolic compounds in food matrices include spectrophotometric and chromatographic procedures,[10,11] whereas flow injection chemiluminescence and electrochemical methods came later on.[12,13] Lately, electrochemical sensors were recognized as more selective, reliable, and sensitive devices over other instrumental tools, with additional advantages such as lower cost, ease of use, and faster response time.[14–16] The electrochemical reaction of the reductant GA on the surface of the electrode is triggered by an applied voltage, which yields a quantifiable current response proportional to the analyte concentration. However, because low kinetics and high over potentials are necessary to oxidize GA, direct oxidation on the surface of the bare electrode is not efficient.[17,18] In addition, recent suggested uses of GA for applications beyond the food sector (*e.g.*, medical, biomedical, and pharmaceutical applications) have imposed the necessity for electrochemical sensors with enhanced selectivity, sensitivity and limit of detection. To this scope, physicochemical modifications on the electrode surface have demonstrated to be the most promising strategy.[19] Sangeetha *et al.* used a graphite electrode modified with thionine and nickel hexacyanoferrate for the determination of gallic acid.[20] They reported a limit of detection of 1.66 μmol L^{-1} and a linear range of 4.99–1200 μmol L^{-1}. In another work, Abdel-Hamid *et al.* fabricated an electrochemical sensor based on the modification of a glassy carbon electrode (GCE) using polyepinephrine for the determination of GA.[13] They calculated

[a]*Department of Food Science and Technology, Yazd Branch, Islamic Azad University, Yazd, Iran*

[b]*DeFENS, Department of Food, Environmental and Nutritional Sciences—Packaging Laboratory (PackLAB), University of Milan, via Celoria 2, 20133 Milan, Italy*

[c]*Department of Textile and Polymer Engineering, Yazd Branch, Islamic Azad University, Yazd, 8916871967, Iran. E-mail: nasirizadeh@iauyazd.ac.ir; Fax: +98 3538211109; Tel: +98 35 38211109*

[d]*Free University of Bolzano, Piazza Università 1, 39100 Bolzano, Italy*

Published on 04 January 2016. Downloaded by Universita Studi di Milano on 28/01/2016 14:32:42.

a detection limit of 0.663 μmol L^{-1} and a linear range of 1–20 μmol L^{-1}. The same authors also claimed the suitability of this sensor for the determination of GA in black tea.

More recently, the use of nanoparticles opened the way for the modification of the electrode surface in order to achieve an enhanced performance of electrochemical sensors. Indeed, nanoparticles possess some unique properties, such as high surface area, strong adsorption ability (*e.g.* of active components, modifiers, *etc.*) and good conductivity.[21] For example, Tashkhourian *et al.* developed a carbon paste electrode modified with TiO_2 nanoparticles for the quantification of GA. They reported 0.94 μmol L^{-1} and 2.5–150 μmol L^{-1} as the detection limit and linear range, respectively. The same authors investigated the application of the modified sensor for detecting the target analyte in green and black tea, demonstrating its suitability to work in real samples.[22] Moreover, silver nanoparticles (AgNPs) seem to have great potential as a modifier for the development of electrochemical sensors due to some main features, such as excellent electrical conductivity, high catalytic activity, and capacitance character.[23]

In the current years, our group has proposed various kinds of electrochemical nano-sensors for the determination of several critical analytes in clinical,[24] industrial,[25] and food fields.[26] In this work, we aimed to develop a new electrochemical sensor for the quantitative determination of GA with higher sensitivity, higher selectivity, and lower limit of detection compared to other electrochemical sensors. To this scope, we decided to use a glassy carbon electrode (GCE) modified with silver nanoparticles, whereas delphinidin was selected as the outer layer in direct contact with the medium due to its chemical structure and redox behaviour in order to enhance the selective oxidation of GA. The rationale behind this strategy was to combine the 'physical' advantages linked to the use of AgNPs and the 'chemical' benefits possibly arising from the immobilization of delphinidin on the AgNPs-modified GC electrode. Full electrochemical characterization of the silver nanoparticle/delphinidin modified glassy carbon electrode (AgNP/Delph/GCE) was carried out and the arising electrochemical properties were described. A potential application of the developed sensor on real food systems was eventually investigated by preliminary trials on a food simulant.

2. Experimental part

2.1. Chemicals and apparatus

Delphinidin chloride (analytical grade ≥95%, molar mass 338.70 g mol^{-1}) was purchased from Sigma Aldrich. Gallic acid (anhydrous, molar mass 170.12 g mol^{-1}), silver nitrate ($AgNO_3$ analytical grade ≥99.8%, molar mass 169.87 g mol^{-1}), nitric acid (HNO_3 solution 1.0 mol L^{-1}) and phosphate buffer solution (0.1 mol L^{-1}, pH 7.0) were purchased from Merck. pH measurements were performed with a Metrohm (Herisau, Switzerland) pH/mV-meter (model 691). Electrochemical experiments were carried out with a μ-Autolab potentiostat PGSTAT 30 (Eco Chemie, Utrecht, Netherlands) coupled with GPES v.4.9 software. Glassy carbon, platinum, and Ag/AgCl electrodes (Azar Electrode Co., Iran) were used, respectively, as working, counter, and reference bare electrodes mounted on the electrochemical cell. All electrochemical experiments were run at 25 ± 2.5 °C under ambient conditions.

2.2. Preparation of modified electrodes

The silver nanoparticle-modified GCE (AgNP/GCE) was prepared by a potential cycling procedure. First, the GCE was polished with alumina abrasive slurry (mean particle size 0.05 μm) on a polishing cloth and then rinsed with double distilled water. The GCE was then modified by a continuous potential cycling from −0.7 to 1.9 V at a sweep rate of 80 mV s^{-1} for 8 cycles in a solution containing 1 mmol L^{-1} $AgNO_3$ and 100 mmol L^{-1} nitric acid.[23] The delphinidin coating was deposited in a second step to eventually obtain the AgNP/Delph/GCE. To do so, the AgNP/GCE was rinsed with double distilled water and then modified by 8 cycles of potential sweep between −100 and 400 mV at 20 mV s^{-1} in a 1.0 mmol L^{-1} solution of delphinidin in a 0.1 mol L^{-1} phosphate buffer solution (pH 7.0). The delphinidin-modified GCE (Delph/GCE) was prepared according to the same procedure used for the AgNP/Delph/GCE preparation, without the silver nanoparticle deposition.

3. Results and discussion

3.1. Electrochemical behaviour of the AgNP/Delph/GCE

Cyclic voltammograms of the AgNP/Delph/GCE in the phosphate buffer and absence of GA at various scan rates from 5 to 4000 mV s^{-1} were acquired, though only the most relevant region from 5 to 175 mV s^{-1} (5 mV s^{-1} scan increment) is shown in Fig. 1. In addition, the inset a is representing the 8 cycles of cyclic voltammograms of potential sweep between −100 and 400 mV at 20 mV s^{-1} in a 1.0 mmol L^{-1} solution of delphinidin in a 0.1 mol L^{-1} phosphate buffer solution (pH 7.0) for making the AgNP/Delph/GCE (inset a). The plot of the anodic and cathodic peak currents (I_{pa} and I_{pc}) *versus* the potential scan rates (inset b) is represented by a straight line ($R^2 = 0.99$ for both I_{pa} and I_{pc}). The electron transport is diffusionless and controlled uniquely by the immobilized delphinidin adsorbed on the electrode surface. This is due to the fact that electron transfer occurs *in situ*, namely on the modified electrode surface. In turn, this confirms the immobilization of the modifier onto the bare glassy carbon electrode (BGCE) surface.[18] For scan rate potentials below 700 mV s^{-1}, the peak-to-peak potential separation ($\Delta E_p = E_{pa} - E_{pc}$) is about 44 mV. This separation reflects a non-Nernstian behaviour. However, this value increased after 700 mV s^{-1} with increasing the scan rates (Fig. 1, insets c and d), showing the limitation arising from the electron transfer kinetics.

Cyclic voltammetry also allowed determining two commonly employed quantities in the kinetic investigation of electrode processes.[27] The apparent heterogeneous electron transfer rate constant, k_s, and the electron transfer coefficient, α, for a surface-confined (*i.e.*, diffusionless) electron transfer between the redox couple of delphinidin and the AgNP/GCE were obtained by plotting the variation of the anodic and cathodic peak potentials *versus* the logarithm of scan rates.[28] Accordingly, k_s,

 This journal is © The Royal Society of Chemistry 2016

Published on 04 January 2016. Downloaded by Universita Studi di Milano on 28/01/2016 14:32:42.

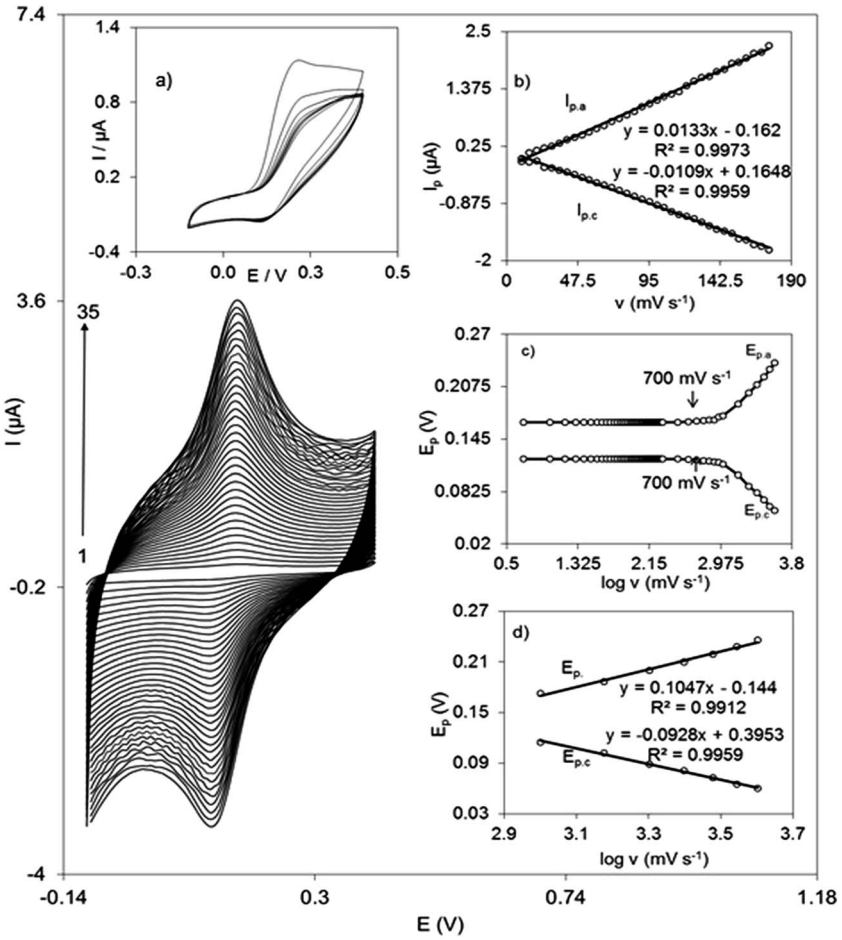

Fig. 1 Cyclic voltammetric responses of the delphinidin modified AgNPs-GCE in 0.1 mol L^{-1} phosphate buffer (pH 7.0) at different scan rates (5–175 mV s^{-1} interval, 5 mV s^{-1} increment). Numbers 1–35 correspond to the scan number. (a) Cyclic voltammograms of 8 cycles of potential sweep between −100 and 400 mV at 20 mV s^{-1} in a 1.0 mmol L^{-1} solution of delphinidin in a 0.1 mol L^{-1} phosphate buffer solution (pH 7.0) for making the AgNP/Delph/GCE. (b) Plots of anodic and cathodic peak currents (I_{pa} and I_{pc}, respectively) *versus* scan rate (5–175 mV s^{-1}); (c) variation of the peak potentials (E_{pa} and E_{pc}) *versus* the logarithm of the scan rate within the (5–4000 mV s^{-1}) range; (d) magnification of the previous plots (1000–4000 mV s^{-1}).

and α can be gathered from the slope and intercept of such plots, respectively. We found that for scan rates above 1 V s^{-1} the E_{pa} and E_{pc} values were proportional to $\log v$ (Fig. 1c). Eventually, $k_s = 13.20$ s^{-1} and $\alpha = 0.55$ were estimated by using Laviron theory. These values reflect the symmetry of the free-energy curve (with respect to the reactants and products) and the excellent attitude of delphinidin to work as an electron transfer mediator for electrocatalytic processes.[26] To assess the potential electrocatalytic oxidation of the different modified electrodes, cyclic voltammetry experiments were carried out using the (a) AgNP/Delph/GCE and (b) Delph/GCE in the absence of GA and (c) AgNP/Delph/GCE, (d) Delph/GCE, (e) AgNP/GCE, and (f) BGCE in the presence of 0.5 mmol L^{-1} GA water solution in 0.1 mol L^{-1} phosphate buffer (pH 7.0). The obtained voltammograms are shown in Fig. 2. Comparing voltammograms Fig. 2(a) and (b) of the AgNP/Delph/GCE and Delph/GCE in the absence of GA, it can be seen that the reversibility of delphinidin at the AgNP/Delph/GCE surface is considerably improved. This effect can be attributed to the

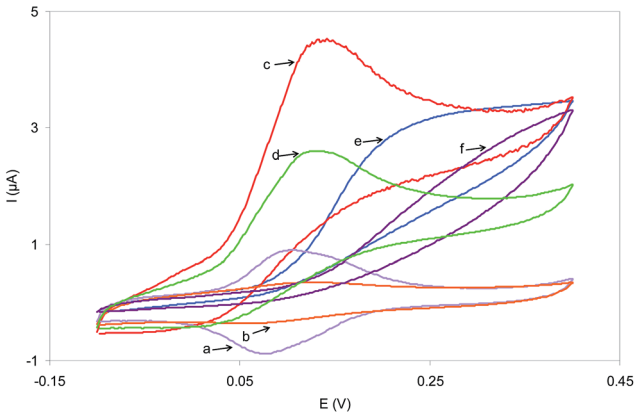

Fig. 2 Cyclic voltammograms in 0.1 mol L^{-1} phosphate buffer (pH 7.0) at a scan rate 20 mV s^{-1} of: (a) AgNP/Delph/GCE and (b) Delph/GCE in the absence GA; (c) AgNP/Delph/GCE, (d) Delph/GCE, (e) AgNP/GCE, and (f) BGCE in the presence of 0.5 mmol L^{-1} GA.

Published on 04 January 2016. Downloaded by Universita Studi di Milano on 28/01/2016 14:32:42.

AgNP deposition, which allowed for a higher surface area of the modified electrode to such an extent that the background voltammetric response and capacitance of the AgNP-coated surface were higher than those of the bare surface. On the other hand, it can be said that the presence of AgNPs on the electrode surface will improve the electron transport between Delph and the GCE. This was clearly demonstrated by the higher current peak, which accounts for an ultimate higher sensitivity of the AgNP/Delph/GCE surface. A comparison between voltammograms (a) and (c) of Fig. 2 reveals that, as expected for electrocatalytic oxidation, there was an increase in the anodic peak current of the AgNP/Delph/GCE$_{ox}$/AgNP/Delph/GCE$_{red}$ redox couple in the presence of GA. Moreover, the cathodic peak current disappeared.

Furthermore, the anodic peak potential associated with the GA oxidation was about 138 mV at the AgNP/Delph/GCE surface (trace c, Fig. 2) and 219 mV at the AgNP/GCE surface (trace e, Fig. 2), while the anodic peak potential recorded for the BGCE (trace f, Fig. 2) was approximately 330 mV. Therefore, the modification made by the electrodeposition of AgNPs yielded a shifting of the peak potential of GA oxidation of 111 mV toward negative values when compared with that at the BGCE. An even better performance was achieved after the immobilization of the delphinidin layer, with a shifting of 192 mV. A lower peak potential is desirable to achieve a better selectivity performance, (*i.e.*, to determine the target analyte in a potential window where a lower number of interferents are present). A similar behaviour was observed when comparing the AgNP/Delph/GCE (trace c, Fig. 2) and the Delph/GCE (trace d, Fig. 2). Again, the presence of the nanoparticles on the electrode surface remarkably enhanced the oxidation peak current of GA due to the increased surface area exposed to the medium. The absence of any cathodic peak for the BGCE and the modified versions indicate that the oxidation product undergoes a further chemical reaction or is not reduced at the glassy carbon electrode.[29] The electrocatalytic oxidation characteristics of GA at various electrode surfaces at pH 7.0 are summarized in Table 1.

Table 1 Comparison of the electrocatalytic oxidation peak potential (E_p) and peak current (I_p) of gallic acid (0.5 mmol L^{-1}) on various electrode surfaces at pH 7.0

Type of electrodes	Oxidation potential (mV)	Oxidation current (μA)
BGCE	330	2.84
AgNP/GCE	219	2.95
Delph/GCE	138	2.59
AgNP/Delph/GCE	138	4.51

3.2. Electrocatalytic oxidation of GA at the AgNP/Delph/GCE

Electrocatalytic oxidation of GA at the AgNP/Delph/GCE surface in a 0.1 mol L^{-1} phosphate buffer solution (pH 7.0) containing 1.50 mmol L^{-1} GA was investigated by cyclic voltammetry

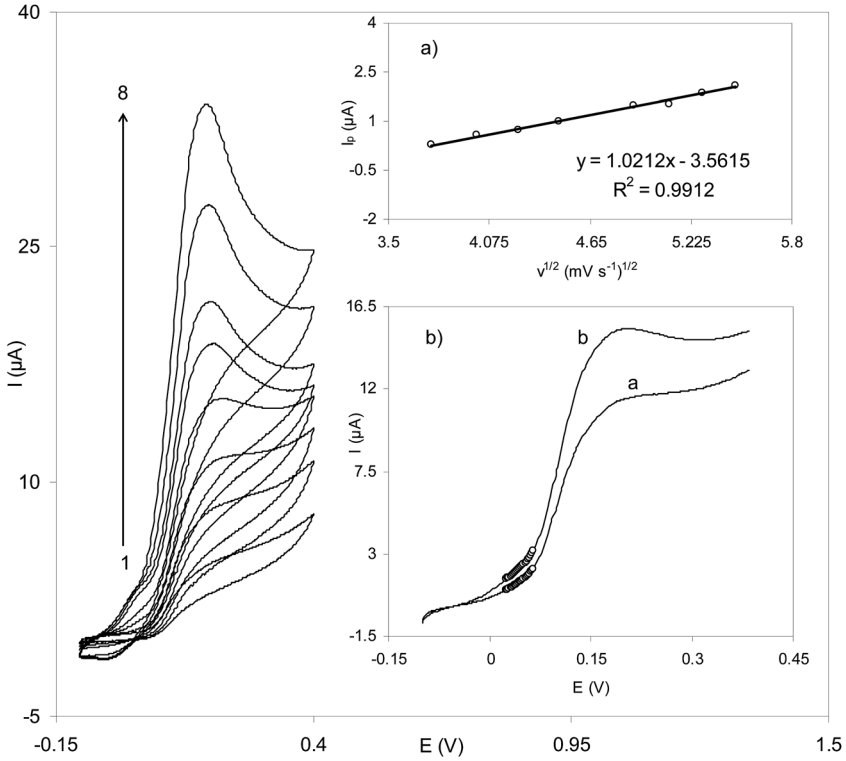

Fig. 3 Cyclic voltammograms of AgNP-Delph-GCE in a 0.1 mol L^{-1} phosphate buffer (pH 7.0) containing 1.50 mmol L^{-1} GA at different scan rates (14, 16, 18, 20, 24, 26, 28, 30 mV s^{-1} interval). (a) Numbers 1–8 correspond to the scan number. The electrocatalytic peak current (I_p) variation as a function of the square root of sweep rate. (b) Sweep voltammogram of AgNPs-Delph-GCE in a 0.l mol L^{-1} phosphate buffer solution (pH 7.0) containing 1.5 mmol L^{-1} GA at 18 (a) and 20 (b) mV s^{-1}.

 This journal is © The Royal Society of Chemistry 2016

Published on 04 January 2016. Downloaded by Universita Studi di Milano on 28/01/2016 14:32:42.

within the scan (sweep) rate range 14–30 mV s^{-1} (Fig. 3). The linear relationship between the electrocatalytic peak current (I_p) and the square root of scan rate ($\nu^{1/2}$) (Fig. 3, inset a) suggests that at an adequate over potential, and according to the eqn (2), the process is diffusion-limited. Consequently the overall electrochemical oxidation of GA at the modified electrode surface might be controlled by the cross-exchange process 'GA ↔ redox site' of the AgNP/Delph/GCE and the diffusion of GA.

Andrieux and Saveant developed a theoretical model that relates the concentration of the analyte and the peak current for low scan rates (14–30 mV s^{-1}) and large values of the kinetic parameters: catalytic rate constant (k'); superficial concentration of the modifier (Γ^0), corresponding to the coverage by one monolayer; and number of equivalent monolayers in the film (l, generally 1 for the usual derivatized electrodes and of the order of 10 and even 100 for redox polymer electrodes):[30]

$$I_{cat} = 0.496nFAC_b(nFD\nu/RT)^{1/2} \quad (1)$$

where n is the number of electrons (2) exchanged per reactant molecule; F is the Faraday constant (9.648×10^4 C mol^{-1}); A is the geometric area of the electrode (0.0314 cm^2); C_b is the bulk concentration of the analyte (mol cm^{-3}); D is the diffusion coefficient of the analyte (1.56×10^{-6} cm^2 s^{-1} obtained by chronoamperometry, see below); ν is the sweep rate (mV s^{-1}); R is the gas constant (8.314 J K^{-1} mol^{-1}); T is the temperature (298 K). Plotting $I_{cat}/nFAC_s(nFD\nu/RT)^{1/2}$ *versus* $\log[lk'\Gamma^0/(nFD\nu/RT)^{1/2}]$ a working curve is then obtained, from which the value of k' can be estimated. According to the above procedure, and based on the data reported by Andrieux and Saveant in Fig. 1 of their paper,[30] an average value of $k' = 7.40 \times 10^{-4}$ cm s^{-1} was eventually estimated for the proposed sensor in the presence of 1.5 mmol L^{-1} of GA for low scan rates (14–30 mV s^{-1}).

By using the slope of the linear plot I_p *versus* $\nu^{1/2}$ (Fig. 3, inset a), the number of electrons (n) involved in the overall catalytic reaction can be gathered according to the following equation for irreversible diffusion-controlled processes.[31]

$$I_p = 3.01 \times 10^5 n[(1-\alpha)n_\alpha]^{1/2}AC_bD^{1/2}\nu^{1/2} \quad (2)$$

where A, C_b, and D have been previously defined and $(1-\alpha)n_\alpha = 0.68$ (see below). The total number of electrons involved in the anodic oxidation of GA was calculated to be $n = 2.21 \cong 2$.

The sweep voltammograms of the AgNP/Delph/GCE in a 0.1 mol L^{-1} phosphate buffer solution (pH 7.0) containing 1.5 mmol L^{-1} of GA obtained at two different scan rates (18 and 20 mV s^{-1}) are reported in (Fig. 3, inset b). The points on the linear sweep voltammograms show that the rising part of the

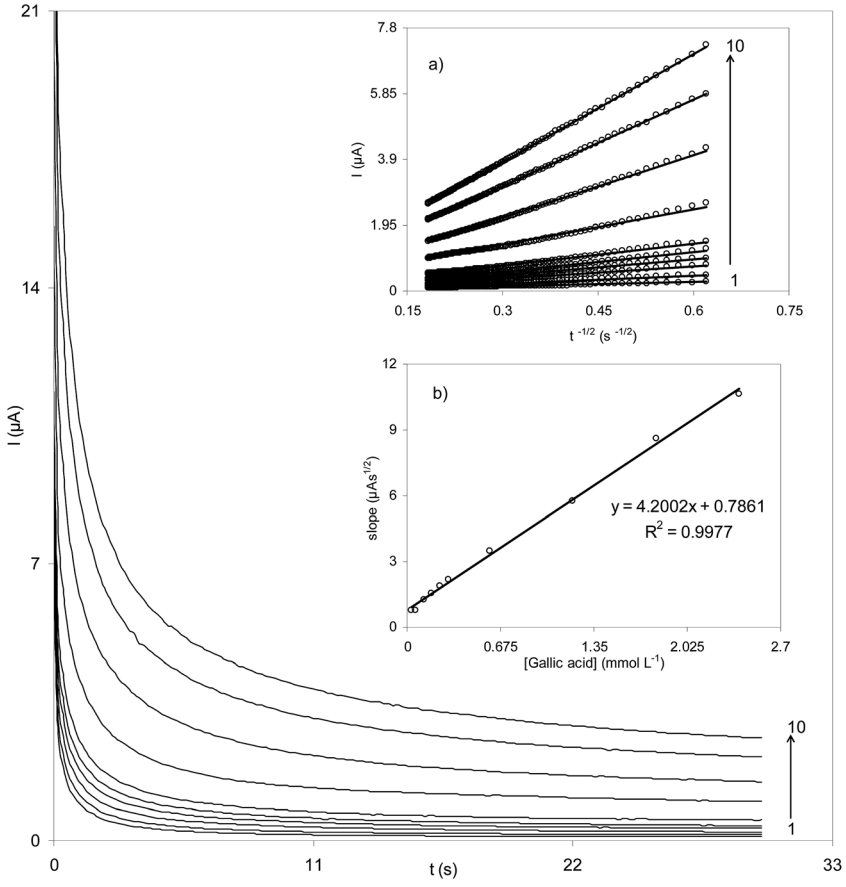

Fig. 4 Current response over time of the AgNP/Delph/GCE in 0.1 mol L^{-1} phosphate buffer solution (pH 7.0) containing different concentrations of GA (0.03, 0.06, 0.12, 0.18, 0.24, 0.3, 0.6, 1.2, 1.8, and 2.4 mmol L^{-1}) during the chronoamperometric measurements (potential 220 mV). Numbers 1–10 correspond to the different GA concentrations. Insets: (a) chronoamperograms of the intensity (I) as a function of the reciprocal square root of time ($t^{-1/2}$); (b) linear plot of the slopes of the ten straight lines in the inset (a) against the GA concentration.

Published on 04 January 2016. Downloaded by Universita Studi di Milano on 28/01/2016 14:32:42.

voltammograms, which is known as the Tafel region, is affected by electron transfer kinetics between the substrate, GA, and the surface-confined delphinidin, assuming the deprotonation of GA as a sufficiently fast step. In this condition, the number of electrons involved in the rate-determining step (*i.e.*, the transfer between GA and the modifier) can be estimated from the slope of the Tafel region.

3.3. Chronoamperometric measurements of electrocatalytic oxidation of GA at the AgNP/Delph/GCE surface

Chronoamperometry experiments at a potential of 220 mV (Fig. 4) made it possible to investigate the catalytic oxidation of GA using the AgNP/Delph/GCE. The current response (I) under a diffusion-controlled electrocatalytic process of an electroactive material (*e.g.*, GA), was described by Cottrell:[21]

$$I = \frac{nFAD^{1/2}C_b}{\pi^{1/2}t^{1/2}} \quad (3)$$

which can be explicated as:

$$D^{1/2} = \frac{\pi^{1/2}}{nFA} \times m \quad (3a)$$

with $m = (It^{1/2})/C_b$. From the raw chronoamperometric traces (I *versus* t), a linear plot for each GA concentration was easily obtained by using the square root of time (Fig. 4, inset a). The slopes of the resulting straight lines were then plotted *versus* the GA concentration to eventually obtain an individual straight line (Fig. 4, inset b), whose slope is m. With n, F, and A known, the average diffusion coefficient (D) of GA was estimated to be 1.56×10^{-6} cm^2 s^{-1}.

3.4. Amperometric studies of electrocatalytic oxidation of GA at the AgNP/Delph/GCE surface

Dynamic amperometry experiments (*i.e.*, conducted by rotating the working electrode) involve a higher current sensitivity than cyclic voltammetry experiments. Therefore, these kinds of experiments can profitably be used to extract the detection limit of GA and measure the linear range at the surface of the working electrode. The amperogram obtained in this work for the rotating AgNP/Delph/GCE is shown in Fig. 5, panel a. The experiments were carried out at a potential of 220 mV in a 0.1 mol L^{-1} phosphate buffer solution (pH 7.0) at different GA concentrations. A linear relationship was found for two wide concentration ranges, *i.e.* 0.60–8.68 μmol L^{-1} (Fig. 5, panel b) and 8.68–625.80 μmol L^{-1} (Fig. 5, panel c).

The linear least square calibration curve of the first range had a slope of 0.01 μA (μmol L^{-1})$^{-1}$ (sensitivity) and a coefficient of determination (R^2) of 0.99. The lower limit of detection, LOD, was obtained according to:[32]

$$\mathrm{LOD} = 3\sigma_{bl}/m \quad (4)$$

where σ_{bl} is the standard deviation of the response obtained from 15 replicates of the blank solution (0.0009), and m is the slope of the calibration plot (0.01 μA (μmol L^{-1})$^{-1}$). A limit of detection of 0.28 μmol L^{-1} was obtained for the GA quantification mediated by the AgNP/Delph/GC electrode. The stability

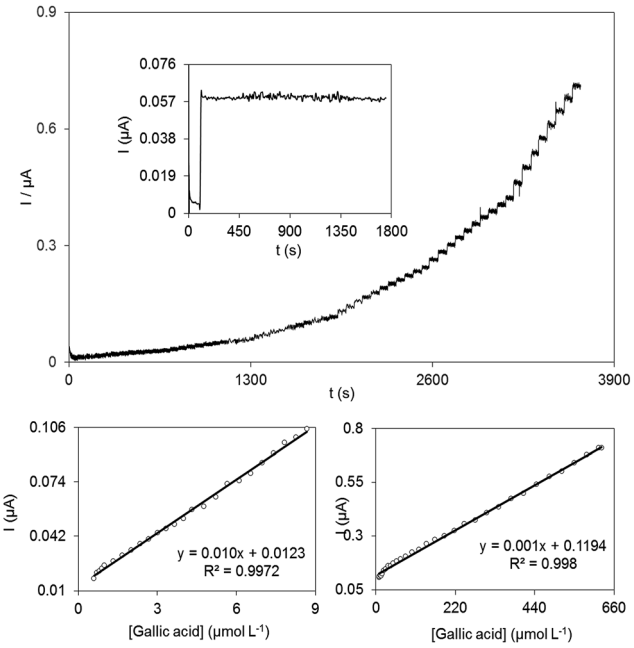

Fig. 5 (a) Amperometric response at rotating AgNP-Delph-GCE held at 220 mV in 10 mL, 0.1 mol L^{-1} phosphate buffer (pH 7) for 0.60–625.80 μmol L^{-1} of gallic acid. The variation of amperometric current *vs.* gallic acid concentration in the range of (panel b) 0.60–8.68 μmol L^{-1} and (panel c) 8.68–625.80 μmol L^{-1}.

of the fabricated sensor in the presence of 5.00 μmol L^{-1} GA over a period of 1750 s is shown in the inset of Fig. 5. The amperometric current of GA did not change and no decrease was observed in the response current. This observation shows that, throughout the monitored time span, there was no inhibition effect due to the adsorption of GA and GA's oxidation products on the modified electrode surface.

Some of the most relevant electroanalytical parameters obtained in this study were compared with those reported in previous studies and are summarized in Table 2.

3.5. Potential determination of GA in beverages

The last part of this study was aimed to assess the suitability of the AgNP/Delph/GCE as an analytical device for the GA determination in real foods. To this goal, 5 mL of different beverage samples (listed in Table 3) were diluted with 10 mL phosphate buffer solution (0.1 mol L^{-1}, pH 7.0). The addition of specific amounts of GA to the cell containing the different beverage samples allowed the determination of the recovery of the analyte. All the measurements presented in Table 3 are performed by measuring the GA oxidation current at the AgNP/Delph/GCE surface and by extrapolation in the calibration graph of Fig. 5. Then, to investigate the concomitant effects of compounds usually present in fruit juices, voltammograms were recorded in the absence and presence of ascorbic acid. It should be noted that the presence of other phenolic acids, if they interacted with Delph, can be considered as an interference agent at determining gallic acid. The final recovery results, in the range

 This journal is © The Royal Society of Chemistry 2016

Published on 04 January 2016. Downloaded by Universita Studi di Milano on 28/01/2016 14:32:42.

Table 2 Comparison of some analytical parameters of the several modified electrodes for gallic acid determination

Electrode	Method	LR[a] (μmol L^{-1})	LOD[b] (μmol L^{-1})	Ref.
Graphite electrode modified with $[Cu_2tpmc](ClO_4)_4$ immobilized in the PVC matrix	DPV[c]	0.25–1, 5–100	0.148	33
Glassy carbon electrode modified with polyepinephrine	DPV	1–20	0.663	13
Graphite electrode modified with thionine and nickel hexacyanoferrate	DPV	4.99–1200	1.66	20
Glassy carbon electrode modified with polyethyleneimine-functionalized graphene oxide	DPV	0.58–58.7	0.41	9
Carbon paste electrode modified with TiO_2 nanoparticles	DPV	2.5–150	0.94	22
AgNP/Delph/GCE	Amperometry	0.60–8.68, 8.68–625.80	0.28	This work

[a] LR = linear range. [b] LOD = limit of detection. [c] DPV = differential pulse voltammetry.

Table 3 Determination of gallic acid in five commercial beverages using the AgNP/Delph/GCE developed in this work

Beverage type	GA added (μmol L^{-1})				GA found (μmol L^{-1})				Recovery (%)			
Apple juice	No addition	10.00	20.00	30.00	19.00	29.20	38.70	49.20	—	100.6	99.23	100.4
Lemon juice	No addition	15.00	30.00	45.00	16.00	31.30	46.10	60.70	—	100.9	100.2	99.50
Peach juice	No addition	5.000	10.00	15.00	12.00	17.00	21.80	27.20	—	100.0	99.09	100.7
Green tea	No addition	20.00	40.00	60.00	25.00	44.90	65.30	85.10	—	99.77	100.4	100.1
Orange juice	No addition	10.00	20.00	30.00	62.00	72.40	81.90	92.50	—	100.5	99.87	100.5

99.09–100.9%, clearly show the potential of the proposed sensor for practical applications, *i.e.* in real food systems.

4. Conclusions

A new electrochemical sensor with a satisfactory limit of detection and high sensitivity was developed for the quantification of the antioxidant phenolic compound GA. The final results obtained within this study provided evidence of the pivotal role played by the AgNPs at the surface of GCE in increasing the sensitivity of the delphinidin coating and the background voltammetric response (capacitance current). In addition, the electrodeposition of delphinidin on the surface of a silver nanoparticle-modified glassy carbon electrode was demonstrated, thus generating an AgNP/Delph/GCE with strong electrocatalytic behaviour (oxidation of GA). Preliminary tests also demonstrated the potential of the developed electrochemical sensor as a valid alternative to the most common analytical techniques for the determination of GA in real food systems.

References

1 M. Becerra-Herrera, M. R. Lazzoi, A. Sayago, R. Beltran, R. Del Sole and G. Vasapollo, *Food Anal. Methods*, 2015, **8**, 2554–2559.
2 A. López-Cobo, A. M. Gómez-Caravaca, J. Švarc-Gajić, A. Segura-Carretero and A. Fernández-Gutiérrez, *J. Funct. Foods*, 2014, **18**, 1167–1178.
3 S. F. Sulaiman and K. L. Ooi, *J. Agric. Food Chem.*, 2014, **62**, 9576–9585.
4 U. Yilmaz, A. Kekillioglu and R. Mert, *J. Anal. Chem.*, 2013, **68**, 1064–1069.
5 R. T. Huang, Y. F. Lu, B. S. Inbaraj and B. H. Chen, *J. Funct. Foods*, 2015, **12**, 498–508.
6 J. D. Hsu, S. H. Kao, T. T. Ou, Y. J. Chen, Y. J. Li and C. J. Wang, *J. Agric. Food Chem.*, 2011, **59**, 1996–2003.
7 L. Fu, B. T. Xu, X. R. Xu, R. Y. Gan, Y. Zhang, E. Q. Xia and H. B. Li, *Food Chem.*, 2011, **129**, 345–350.
8 Z. Yang, D. Zhang, H. Long and Y. Liu, *J. Electroanal. Chem.*, 2008, **624**, 91–96.
9 J. H. Luo, B. L. Li, N. B. Li and H. Q. Luo, *Sens. Actuators, B*, 2013, **186**, 84–89.
10 D. A. Kostic, S. S. Mitic, M. N. Mitic and S. M. Sunaric, *Oxid. Commun.*, 2012, **35**, 153–159.
11 P. A. Pednekar, V. Kulkarni and B. Raman, *Asian J. Pharm. Clin. Res.*, 2014, **7**, 86–89.
12 S. Li, H. Sun, D. Wang, L. Qian, Y. Zhu and S. Tao, *Chin. J. Chem.*, 2012, **30**, 837–841.
13 R. Abdel-Hamid and E. F. Newair, *J. Electroanal. Chem.*, 2013, **704**, 32–37.
14 W. Gu, M. Wang, X. Mao, Y. Wang, L. Li and W. Xia, *Anal. Methods*, 2015, **7**, 1313–1320.
15 L. Lin, H. T. Lian, X. Y. Sun, Y. M. Yu and B. Liu, *Anal. Methods*, 2015, **7**, 1387–1394.
16 X. Tan, J. Wu, Q. Hu, X. Li, P. Li, H. Yu, X. Li and F. Lei, *Anal. Methods*, 2015, **7**, 4786–4792.
17 M. Kahl and T. M. Golden, *Electroanalysis*, 2014, **26**, 1664–1670.
18 A. J. Bard and L. R. Faulkner, *Electrochemical Methods: Fundamentals and Applications*, Wiley, New York, 2nd edn, 2000.
19 J. Wang, *Electroanalysis*, 1991, **3**, 255–259.
20 N. S. Sangeetha and S. S. Narayanan, *Anal. Chim. Acta*, 2014, **828**, 34–45.
21 H. Gao, X. Qi, Y. Chen and W. Sun, *Anal. Chim. Acta*, 2011, **704**, 133–138.

Published on 04 January 2016. Downloaded by Universita Studi di Milano on 28/01/2016 14:32:42.

22 J. Tashkhourian, S. F. N. Ana, S. Hashemnia and M. R. Hormozi-Nezhad, *J. Solid State Electrochem.*, 2013, **17**, 157–165.
23 N. Nasirizadeh, M. M. Aghayizadeh, S. M. Bidoki and M. E. Yazdanshenas, *Int. J. Electrochem. Sci.*, 2013, **8**, 11264–11277.
24 N. Nasirizadeh, Z. Shekari, M. Tabatabaee and M. Ghaani, *J. Braz. Chem. Soc.*, 2015, **26**, 713–722.
25 H. R. Zare and N. Nasirizadeh, *Electrochim. Acta*, 2007, **52**, 4153–4160.
26 N. Nasirizadeh, S. Hajihosseini, Z. Shekari and M. Ghaani, *Food Anal. Methods*, 2015, **8**, 1546–1555.
27 R. Guidelli, R. G. Compton, J. M. Feliu, E. Gileadi, J. Lipkowski, W. Schmickler and S. Trasatti, *Pure Appl. Chem.*, 2014, **86**, 245–258.
28 E. Laviron, *J. Electroanal. Chem. Interfacial Electrochem.*, 1979, **101**, 19–28.
29 P. A. Kilmartin, H. Zou and A. L. Waterhouse, *J. Agric. Food Chem.*, 2001, **49**, 1957–1965.
30 C. P. Andrieux and J. M. Saveant, *J. Electroanal. Chem. Interfacial Electrochem.*, 1978, **93**, 163–168.
31 S. Antoniadou, A. D. Jannakoudakis and E. Theodoridou, *Synth. Met.*, 1989, **30**, 295–304.
32 D. A. Skoog, F. J. Holler and S. R. Crouch, *Principles of Instrumental Analysis*, Thomson Brooks/Cole, London, 6th edn, 2007.
33 B. B. Petkovic, D. Stankovic, M. Milcic, S. P. Sovilj and D. Manojlovic, *Talanta*, 2015, **132**, 513–519.

This journal is © The Royal Society of Chemistry 2016